

## Graphene-Supported Pt-Based Intermetallic as Highly Efficient Catalysts in Fuel Cells

L.Z. ZHENG\*, K. HAN, L.Y. XIONG, Z.J. ZOU, K. TAO and D. YE

Department of Chemistry and Chemical Engineering, East China Jiaotong University, NanChang 330013, P.R. China

\*Corresponding author: Tel: +86 791 87046351; E-mail: zhenglongzhen@tsinghua.org.cn; 644453303@qq.com

(Received: 30 June 2012;

Accepted: 29 April 2013)

AJC-13404

Graphene-supported Pt and Pt<sub>x</sub>M<sub>y</sub> (M = Fe, Co and Cu) intermetallic catalysts are prepared by thermal treatment approach and characterized with X-ray diffraction, scanning electron micrographs and rotating disk electrode. Electrocatalytic performance of the prepared materials revealed that they have higher catalytic activity and stability than commercial Pt/C for both the ethanol oxidation reaction and the oxygen reduction reaction in direct alcohol fuel cells. The enhanced electrocatalytic performance of the prepared catalysts is attributed to the Pt alloyed with transition metal (Fe, Co and Cu), which changes both the geometric and electronic structures of Pt in the solution. Therefore, from the electrochemical, morphological and compositional results, it has demonstrated that a better performance of ethanol oxidation reaction and oxygen reduction reaction could be realized at the graphene-supported Pt-based intermetallic catalysts.

**Key Words:** Graphene, Intermetallic, Catalysts, Ethanol oxidation reaction, Oxygen reduction reaction.

### INTRODUCTION

Direct alcohol fuel cells are of growing interest due to their ease of handling, high-energy densities and low pollution for a wide range of applications<sup>1</sup>. The Pt-based catalyst for both the anode and the cathode is currently one of the key components in fuel cells<sup>2,3</sup>, which accounts for a large sum of expenses in the total cost of fuel cell manufacturing. In order to achieve durable and active catalysts with a low cost, considerable efforts have been developed for the development of Pt-based or alternative catalysts<sup>4-6</sup>. In recent years, more and more people focused on fabrication, processing and characterization of Pt-based bimetallic nanoparticles with controllable size (1-10 nm), shape, composition and morphology (e.g. heterostructure, core@shell and intermetallic)<sup>7-11</sup>. Among these catalysts, the added metals can notably enhance the catalytic activity, improving the stability and reduce the use of Pt by the changes of electronic effects, the surface binding sites and the lattice<sup>12</sup>.

General speaking, the different composition we choose is usually correlated with the catalytic behaviour of bimetallic catalysts; the distribution of each element within the catalyst is also found to have significant effects on the electrocatalytic activity and durability of catalysts<sup>13,14</sup>. Nowadays, many methods have been developed on Pt<sub>x</sub>M<sub>y</sub> (M = Fe, Co, Cu, etc.) bimetallic catalysts (especially for heterostructure and core@shell), the results have shown that they are more active for the electrochemical reduction of molecular oxygen than

pure Pt.<sup>15,16</sup> However, the prepared catalysts are usually protected by organic substance or surfactant, which is bad to enhance the activity of these catalysts. Such insight to corresponding nanoscale alloy materials is still lacking. Moreover, catalyst durability is highly dependent on the homogeneous mixture of two metal atoms and their compositional profiles<sup>17,18</sup>. The controllable synthesis of intermetallic is much more complicated and difficult to be achieved<sup>19,20</sup>. Pt-based intermetallic catalysts prepared by conventional methods usually possess some organic compounds or protective agent and the catalytic performance is compromised<sup>21,22</sup>. Therefore, a synthetic approach toward homogeneous intermetallic catalysts is needed to achieve efficient advancement and perfection of the catalytic properties in direct alcohol fuel cells systems.

Here we introduce the synthesis of monodisperse and highly homogeneous graphene-supported Pt-based catalysts with 25 wt. % metal loading. To achieve even distribution of elements, we use thermal treatment approach to synthesize homogeneous Pt<sub>x</sub>M<sub>y</sub> (M = Fe, Co and Cu) intermetallic catalysts; followed by the chemical dealloying process which resulted a porous structure in the surface. The performance of obtained catalysts is compared with commercial Pt/C (E-TEK) under the same conditions.

### EXPERIMENTAL

**Functionalization of graphene:** The procedure for the polyelectrolyte functionalization of graphene with poly (diallyl

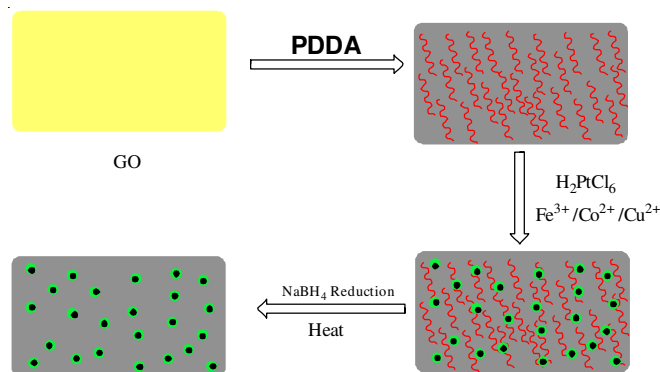
dimethyl ammonium chloride) is briefly described as follows. Graphene oxide was first prepared from natural graphite powder through a modified Hummers' method<sup>23,24</sup>. 60 mg of graphene oxide powder in 30 mL of H<sub>2</sub>O was sonicated for 1 h to form a homogeneous graphene oxide suspension, 90 mL of H<sub>2</sub>O and 2 mL of 20 wt. % poly (diallyl dimethyl ammonium chloride) solutions was mixed with the graphene oxide suspension under vigorous stirring for 15 min. Then the solution was heated in refluxing conditions at 90 °C for 5 h. During this process, the colour of the solution changed from yellow to black. The resulting graphene suspension was filtering through a Millipore filter (40 mm in diameter and 0.45 µm in pore size), followed by washing with plenty of distilled water, peeling off from the filter and redispersed in water.

*In situ* synthesis of Pt-based intermetallic on poly (diallyl dimethyl ammonium chloride) functionalized graphene first, graphene-supported Pt<sub>x</sub>M<sub>y</sub> (M = Fe, Co and Cu) catalysts with 25 wt. % metal loading were synthesized at room temperature. In a typical synthesis, stoichiometric amounts of anhydrous H<sub>2</sub>PtCl<sub>6</sub> and FeCl<sub>3</sub> (CoCl<sub>2</sub>/CuCl<sub>2</sub>) were dispersed in 20 mL of poly (diallyl dimethyl ammonium chloride)-graphene (0.5 mg/mL). After being stirred for about 15 min, the fresh prepared NaBH<sub>4</sub> solution was added dropwise and stirred for 12 h. The products were collected by centrifugation or dry immediately. Then the obtained black products were annealed in H<sub>2</sub> at 700-800 °C for 8 h.

The XRD pattern was collected on a Bruker D<sub>8</sub> Advance X-ray diffractometer using X radiation. The samples for XRD were prepared by placing a drop of colloidal solution on a clean glass plate. Electrochemical activities were measured by using a three-electrode electrochemical cell and a rotating disk electrode. A saturated Ag/AgCl electrode and a Pt wire were used as reference and counter electrodes, respectively.

## RESULTS AND DISCUSSION

The whole procedure for the synthesis of graphene-supported Pt based intermetallic catalysts are shown in **Scheme-I**. We studied three different graphene-supported Pt<sub>x</sub>M<sub>y</sub> (M = Fe, Co and Cu) intermetallic catalysts with different molar ratios. The focus of the present study is placed on the homogeneity and elemental distribution within the composites.



**Scheme-I:** Procedure to design Graphene-supported Pt based intermetallic catalysts

Fig. 1 is the XRD patterns of the prepared graphene-Pt<sub>3</sub>Fe catalyst. The absence of peaks for pure metal crystal phases

demonstrates the uniform distribution of atoms within the catalysts. This indicates the 3d transition metal atoms were equally distributed in the Pt lattice and reduced Pt-Pt bond lengths. All the reflections of the sample were kept consistent with the JCPDS. All of these evidences reveal that these catalysts possess a uniform intermetallic structure. The obtained highly homogeneous intermetallic catalysts have led into a systematic analysis of the electrocatalytic performance of such Pt-based catalyst systems.

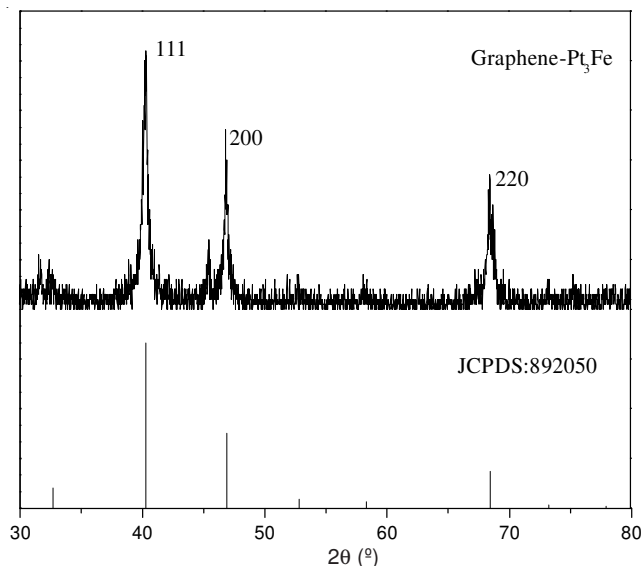


Fig. 1. X-ray diffraction patterns of graphene-Pt<sub>3</sub>Fe intermetallic catalyst

In order to perform electrochemical characterization, the intermetallic catalysts were first placed in acid solution to dissolve the transition metals on the surface of catalysts. It is helpful to form a porous Pt skin while the core retained the intermetallic structure. After this step, the obtained intermetallic composites can be applied as catalysts. The graphene-supported intermetallic catalysts were examined using cyclic voltammetry and rotating disk electrode methods for assessing their electrocatalytic activity and stability for ethanol oxidation reaction and oxygen reduction reaction. The catalysts were mixed with Nafion in ethanol to prepare the catalyst inks that were loaded on the glassy carbon electrode. The kinetic current from the rotating disk electrode data provide quantitative measures for assessing the electrocatalytic activities in term of their correlation with the composition, size and morphology.

In Fig. 2, the cyclic voltammetry measurements of ethanol oxidation reaction were carried out in EtOH (0.1 M)-H<sub>2</sub>SO<sub>4</sub> (0.1 M) aqueous solution at room temperature. The solutions were bubbled with N<sub>2</sub> gas for 0.5 h to remove O<sub>2</sub> before the cyclic voltammetry measurements. Compared with commercial Pt/C catalyst, the graphene-Pt<sub>x</sub>Fe<sub>y</sub> catalyst shows much higher catalytic activity, the forward and backward anodic peak of graphene-Pt<sub>x</sub>Fe<sub>y</sub> has negative shifted of -25 mV. The peak current is also enhanced with the increase of Pt content in the graphene-Pt<sub>x</sub>Fe<sub>y</sub> catalyst and reaches the best values at a Pt/Fe molar ratio of 3:1. However, the electrocatalytic activity changes little when further increasing the Pt/Fe molar ratio.

In order to clarify the role of graphene in the graphene-Pt<sub>x</sub>Fe<sub>y</sub> catalyst, we studied the electrocatalytic activity of

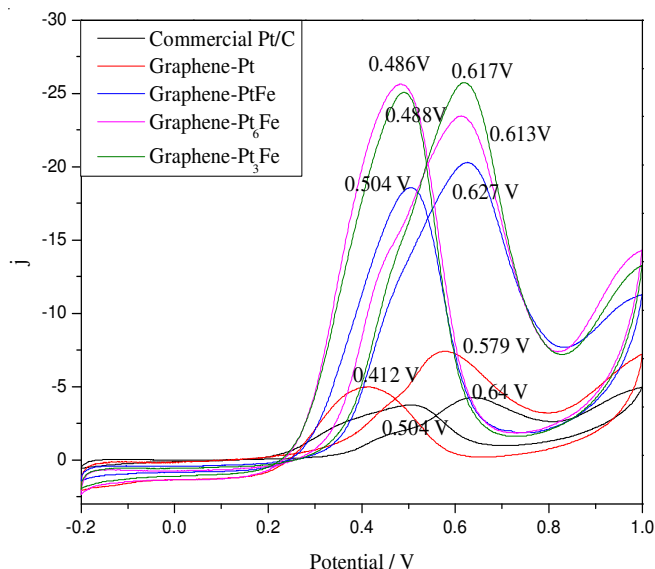


Fig. 2. Cyclic voltammetry curves of Graphene-Pt<sub>y</sub>Fe<sub>y</sub> intermetallic catalyst in EtOH (0.1 M) - H<sub>2</sub>SO<sub>4</sub> (0.1 M) aqueous solution saturated with N<sub>2</sub>. The scanning rate of the applied voltage is 10 mV/s

graphene-Pt towards the ethanol oxidation reaction and compared with commercial Pt/C. It was found that the graphene-Pt catalyst has similar cyclic voltammetry features (such as the anodic current and shapes of the ethanol oxidation reaction peaks) with commercial Pt/C catalyst. However, the anodic peaks of graphene-Pt are observed at about 0.58 V in the forward sweep and 0.41 V in the backward sweep, which remarkable negatively shifted compared to commercial Pt/C. It shows that the structures and properties of the catalyst support have a great effect on the activity and durability of the catalysts; these results are in good agreement with the reports<sup>25,26</sup>. This result highlights the importance of electrical conductivity of graphene supports to the overall direct alcohol fuel cells performance of anodic catalysts.

The stability of the commercial Pt/C and graphene-Pt<sub>3</sub>Fe catalysts for ethanol oxidation reaction was tested in EtOH (0.1 M)-H<sub>2</sub>SO<sub>4</sub> (0.1 M) aqueous solution at an applied initial voltage of 0.7 V for 30 min. As shown in Fig. 3, the current of the graphene-Pt<sub>3</sub>Fe intermetallic catalyst is nearly 2.5 times higher than that of the commercial Pt/C and it also decays more slowly in the later time.

Fig. 4 shows the I-V curves related to the oxygen reduction reaction process for the obtained graphene-Pt<sub>3</sub>Fe intermetallic catalyst. At the half-wave potential, the oxygen reduction reaction current densities generated by the graphene-Pt and the graphene-Pt<sub>3</sub>Fe intermetallic catalysts have greatly enhanced than the commercial Pt/C catalyst. We observed that both Pt/C and graphene-Pt have similar oxygen reduction reaction onset potentials, but the graphene-Pt<sub>3</sub>Fe catalyst has positive shifts of -50 mV.

Apart from graphene-Pt<sub>3</sub>Fe intermetallic catalyst, we also developed some other catalysts (graphene-PtCo<sub>1.45</sub> and graphene-Pt<sub>3</sub>Cu). In Fig. 5, we observed that these catalysts could also enhance the oxygen reduction reaction current densities and reduce onset potentials by closely 20 mV. It indicated that the intermetallic structure is very helpful to the electrocatalytic reactions.

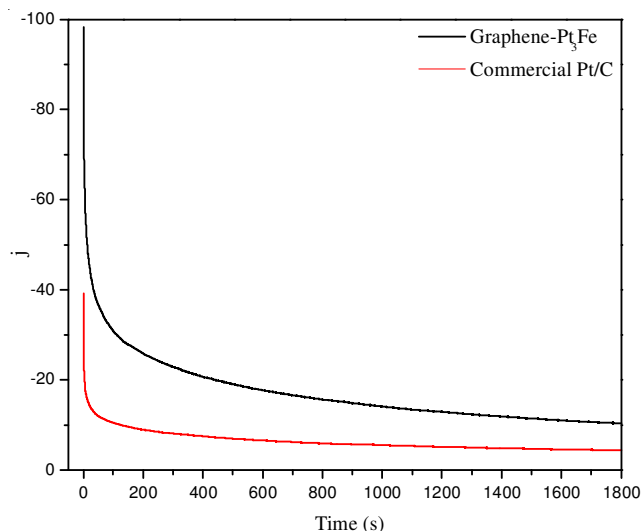


Fig. 3. I-t curves for graphene-Pt<sub>3</sub>Fe intermetallic and commercial Pt/C catalyst in EtOH (0.1 M) - H<sub>2</sub>SO<sub>4</sub> (0.1 M) at an applied voltage of 0.7 V

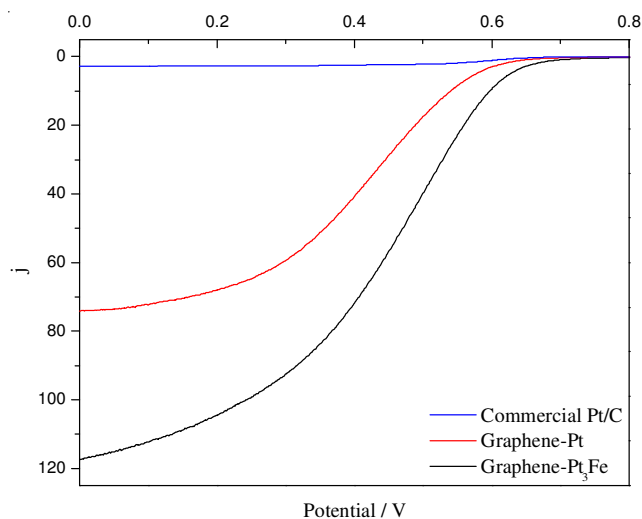


Fig. 4. Rotating disk electrode curves of graphene-Pt<sub>3</sub>Fe intermetallic, graphene-Pt and commercial Pt/C catalysts in H<sub>2</sub>SO<sub>4</sub> (0.5 M) saturated with O<sub>2</sub>. Scanning rate: 10 mV/s. r = 2500 rpm

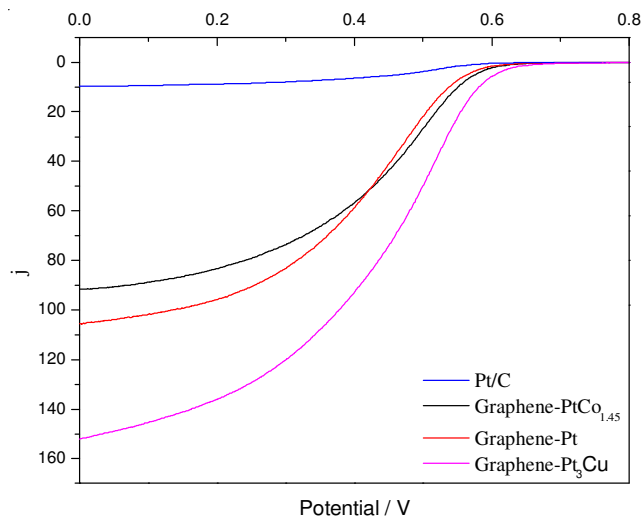


Fig. 5. Rotating disk electrode curves of graphene-Pt<sub>M</sub> (M=Co and Cu) intermetallic, graphene-Pt and commercial Pt/C catalysts in O<sub>2</sub> saturated HClO<sub>4</sub> (0.1 M). Scanning rate: 10 mV/s. r = 2500 rpm

The observed ethanol oxidation reaction and oxygen reduction reaction enhancement by the graphene-Pt<sub>x</sub>M<sub>y</sub> (M = Fe, Co and Cu) is attributed to the Pt alloyed with transition metal, which changes both the geometric and electronic structures of Pt in the solution. The synergic effect in intermetallic catalysts is helpful to improve catalytic properties. It is suggested that the porous Pt shell could supply high electrochemical surface area, thus leading to high electrocatalytic activity.

### Conclusion

In summary, this work explores a unique feature of graphene-Pt<sub>x</sub>M<sub>y</sub> (M = Fe, Co and Cu) intermetallic catalysts and systematically compared the effects of the composition and molar ratio toward electrocatalytic activity in direct alcohol fuel cells. These catalysts have higher direct alcohol fuel cells activities than the commercial Pt/C catalyst. The results highlight the importance of intermetallic structure in catalyst. The developed methods can be a useful approach for preparing graphene-supported Pt-based intermetallic catalysts, which could be potentially useful in large-scale production of cost-effective and highly efficient direct alcohol fuel cells.

### ACKNOWLEDGEMENTS

The project was supported by the National Natural Science Foundation of China (20965003, 21163007, 21165009).

### REFERENCES

1. L. Carrette, K.A. Friedrich and U. Stimming, *Fuel Cells*, **1**, 5 (2001).
2. Y.L. Hsin, K.C. Hwang and C.T. Yeh, *J. Am. Chem. Soc.*, **129**, 9999 (2007).
3. K. Junhyung, W.L. Seung, C. Christopher and S.H. Yang, *J. Phys. Chem. Lett.*, **2**, 1332 (2011).
4. A. Kloke, F.V. Stetten, R. Zengerle and S. Kerzenmacher, *Adv. Mater.*, **23**, 4976 (2011).
5. M.U. Sreekuttan, M.D. Vishal, K.P. Vijayamohan and K. Sreekumar, *J. Phys. Chem. C.*, **114**, 14654 (2010).
6. H.R. Byon, J. Suntivich and S.H. Yang, *Chem. Mater.*, **23**, 3421 (2011).
7. V. Stamenkovic, T.J. Schmidt, P.N. Ross and N.M. Markovic, *J. Phys. Chem. B*, **106**, 11970 (2002).
8. J. Zhang, Y. Mo, M.B. Vukmirovic, R. Klie, K. Sasaki and R.R. Adzic, *J. Phys. Chem. B*, **108**, 10955 (2004).
9. S. Mukerjee, S. Srinivasan, M.P. Soriaga and J. McBreen, *J. Electrochem. Soc.*, **142**, 1409 (1995).
10. J. Zhang, M.B. Vukmirovic, K. Sasaki, A.U. Nilekar, M. Mavrikakis and R.R. Adzic, *J. Am. Chem. Soc.*, **127**, 12480 (2005).
11. K.M. Bratlje, H. Lee, K. Komvopoulos, P. Yang and G.A. Somorjai, *Nano Lett.*, **7**, 3097 (2007).
12. P. Strasser, S. Koh, T. Anniyev, J. Greeley, K. More, C.F. Yu, Z.C. Liu, S. Kaya, D. Nordlund, H. Ogasawara, M.F. Toney and A. Nilsson, *Nature Chem.*, **2**, 454 (2010).
13. E. Antolini, J.R.C. Salgado and E.R. Gonzalez, *J. Power Sour.*, **160**, 957 (2006).
14. S. Mukerjee, S. Srinivasan, M.P. Soriaga and J. McBreen, *J. Electrochem. Soc.*, **142**, 1409 (1995).
15. B.S. Mun, M. Watanabe, M. Rossi, V. Stamenkovic, N.M. Markovic and J. Ross, *J. Chem. Phys.*, **123**, 204717 (2005).
16. F. Hasche, M. Oezaslan and P. Strasser, *ChemCatChem.*, **3**, 1805 (2011).
17. A. Morozan, B. Josselme and S. Palacin, *Energy Environ. Sci.*, **4**, 1238 (2011).
18. C.J. Zhong, J. Luo, B. Fang, B.N. Wanjala, P.N. Njoki, R. Loukrakpam and J. Yin, *Nanotechnology*, **21**, 062001 (2010).
19. D.S. Wang and Y.D. Li, *Adv. Mater.*, **23**, 1044 (2011).
20. R. Hao, R.J. Xing, Z.C. Xu, Y.L. Hou, S. Gao and S.H. Sun, *Adv. Mater.*, **22**, 2729 (2010).
21. D.S. Wang, P. Zhao and Y.D. Li, *Scientific Reports*, **1**, 37 (2011).
22. S.H. Zhou, B. Varughese, B. Eichhorn, G. Jackson and K. McIlwrath, *Angew. Chem.*, **117**, 4615 (2005).
23. W.S. Hummers Jr. and R.E. Offeman, *J. Am. Chem. Soc.*, **80**, 1339 (1958).
24. X.B. Yan, J.T. Chen, J. Yang, Q.J. Xue and P. Miele, *Appl. Mater. Interf.*, **2**, 2521 (2010).
25. Y.C. Xing, L. Li, C.C. Chusuei R. and V. Hull, *Langmuir*, **21**, 4185 (2005).
26. J.J. Wang, G.P. Yin, Y.Y. Shao, Z.B. Wang and Y.Z. Gao, *J. Phys. Chem. C*, **112**, 5784 (2008).